Available online at www.sciencedirect.com

SciVerse ScienceDirect

Ceramics International 38 (2012) 5243–5250

CERAMICS INTERNATIONAL

www.elsevier.com/locate/ceramint

Structural, dielectric and ferroelectric properties of SBN ceramics synthesized by microwave reactive sintering technique

S.N. Kumar [a], P. Kumar [a,*], D.K. Agrawal [b]

[a] Department of Physics, National Institute of Technology, Rourkela 769008, India

[b] Materials Research Institute, The Pennsylvania state University, University Park, PA 16802, USA

Received 21 January 2012; received in revised form 13 March 2012; accepted 13 March 2012

Available online 21 March 2012

Abstract

Strontium barium niobate ($Sr_xBa_{1-x}Nb_2O_6$ with $x = 0.53$/SBN53) ceramics have been synthesized by microwave reactive sintering technique. Powders corresponding to SBN53 stoichiometric composition were calcined at 1200 °C for 20, 30 and 45 min; and the green pellets made of calcined powders were sintered at 1300 °C for 20, 30 and 40 min in a microwave furnace. Ceramics with tungsten bronze type crystal structure were obtained in relatively much less processing time as compared to conventional processing. The reaction between strontium niobate (SN) and barium niobate (BN) phases present in the calcined powders enhances the densification process of the ceramics during sintering. A relative density ~98.3% was obtained in SBN53 ceramics sintered for 40 min. Curie transition temperature (T_c) and dielectric constant (ε_r) were found to vary from 113 to 135 °C and from 1350 to 2500, respectively, depending on the processing conditions.

Keywords: A. Microwave processing; C. Dielectric properties; C. Ferroelectric properties; Reactive sintering

1. Introduction

The tungsten bronze structure based ferroelectrics are a large class of technically important functional materials [1]. The system strontium barium niobate, $Sr_xBa_{1-x}Nb_2O_6$ (SBN) for $x = 0.32$–0.82 is found to exist in tetragonal tungsten bronze (TTB) structure [2]. SBN has many technological applications such as electro-optic, pyroelectric, holographic data storage, piezoelectric, and photorefractive devices because of its excellent pyroelectric [3,4] and linear electro-optic effects with low half-wave voltage and photo refractive sensitivity [5–9]. In addition, it has the advantage of being lead-free material, an important aspect from environment, safety and health view point [10]. The properties of SBN are very sensitive to the amount and type of substitution, method of preparation and sintering conditions [2,11]. In many applications, SBN ceramics, with high density and uniform microstructure are desirable [12]. Techniques like hot-pressing [13], double stage sintering [14], usage of sintering aids [15], templated grain growth [16], reactive sintering [17], microwave processing [18], etc. are used to obtain high density in polycrystalline ceramics of SBN system.

Generally, conventional solid state reaction route, involves two stages of heating. First is the calcination of powders to obtain the single phase and then heating the calcined powders for densification i.e. sintering. Whereas, reactive sintering involves a single stage of heating of either the constituent oxides or intermediate products [19]. Reactive sintering involves both chemical reaction and densification in a single heat treatment. The two steps can be simultaneous or in sequence, depending on the material and processing variables [20]. The free energy of the chemical reaction among the reactants provides an additional driving force for sintering and therefore higher densification. However, reactive sintering is very sensitive to processing conditions such as heating rate, homogeneity of the precursors, density of green compact and particle size of precursors. During slow heating, solid state diffusion can generate intermediate phases which inhibit the subsequent reaction leading to porosity in the material [21].

Presently, the microwave processing of materials is being extensively used because of its many advantages such as enhancement in sintering, fine and uniform microstructure

* Corresponding author.
E-mail address: pvn77@rediffmail.com (P. Kumar).

0272-8842/$36.00
doi:10.1016/j.ceramint.2012.03.034

leading to better properties; environmentally friendly and economic advantages through the saving of energy, space, and time [22]. In the microwave processing heat is generated internally within the material instead of originating from external sources (as in conventional processes), and hence there is an inverse heating profile. The heating is very rapid and homogeneous as the material is heated by energy conversion rather than by energy transfer which occurs in conventional techniques resulting in large thermal gradients. Microwave heating is a function of the material being processed, when the material is microwave sensitive (material with permanent electric dipoles) energy losses are lesser compared to processing of the same material by conventional heating. The homogeneous and fast heating of the ceramics by microwave assisted heating can avoid micro cracks, internal stresses, Kirkendall effect, etc.

In this work, $Sr_{0.53}Ba_{0.47}Nb_2O_6$ (SBN53) ceramics have been prepared by microwave processing. Microwave processing has been used for both calcination and sintering steps of SBN53 ceramics. Effect of microwave reactive sintering process on density, structure, morphology and dielectric properties of SBN53 have been investigated and discussed in detail.

2. Experimental procedure

$SrNO_3$ (99%), $BaNO_3$ (99%) and Nb_2O_5 (99.9%) (Merck, India) precursors in stoichiometric proportion were used for the synthesis of SBN53 samples. The stoichiometric proportions of these precursors were ball milled for 10 h using zirconia balls in acetone medium. The slurry was air dried at room temperature (RT) and then the powder was manually grinded for 1 h in an agate mortar. The powders were calcined at 1200 °C for different times i.e. 20, 30 and 45 min in the laboratory type microwave furnace, shown in Fig. 1. It is a multimode, 2.45 GHz and maximum 3 kW power furnace. In the calcined powders, 3 wt% PVA binder solution was added and by using

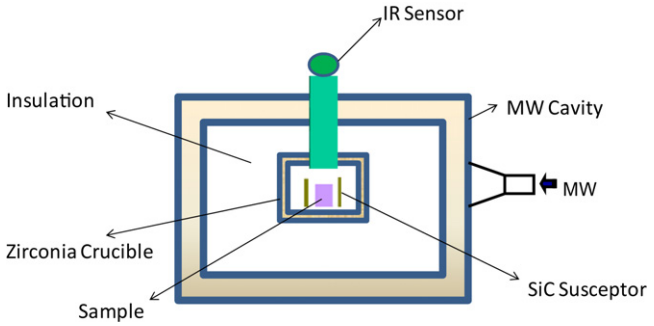

Fig. 1. Schematic diagram of microwave sintering system.

hydraulic press pellets of diameter ~10 mm and thickness ~1.5 mm were formed by using a pressure ~6.5 MPa. The different green compacts were sintered at 1300 °C for 20, 30 and 40 min in microwave furnace. For simplicity SBN-*x*–*y* was used to represent the SBN53 ceramics, where *x* referred to calcination time (at 1200 °C) and *y* referred to sintering time (at 1300 °C) i.e. SBN-20–30 means SBN53 ceramic prepared from powder calcined at 1200 °C for 20 min and sintered for 30 min at 1300 °C. The phase analysis of the calcined powder and sintered pellets was carried out using XRD (Philips, PW 3020) with Cu Kα radiation (λ = 1.5405 Å). The microstructure of sintered samples was examined using Jeol JSM-6480 scanning electron microscope (SEM). Density of the sintered samples was measured by the Archimedes principle using kerosene as the displacement fluid. The sintered ceramic samples were polished and manually coated with silver paste for electric measurements. Silver coated ceramic samples were annealed at 200 °C for 1 h for good adhesion. Relative dielectric constant (ε_r), dielectric loss (tan δ) and impedance (Z) were measured as a function of temperature using computer interfaced Hioki 3532-50 LCR HiTESTER. Polarization as a function of electric field (P–E hysteresis loops) was measured using computer interfaced Sawyer–Tower circuit.

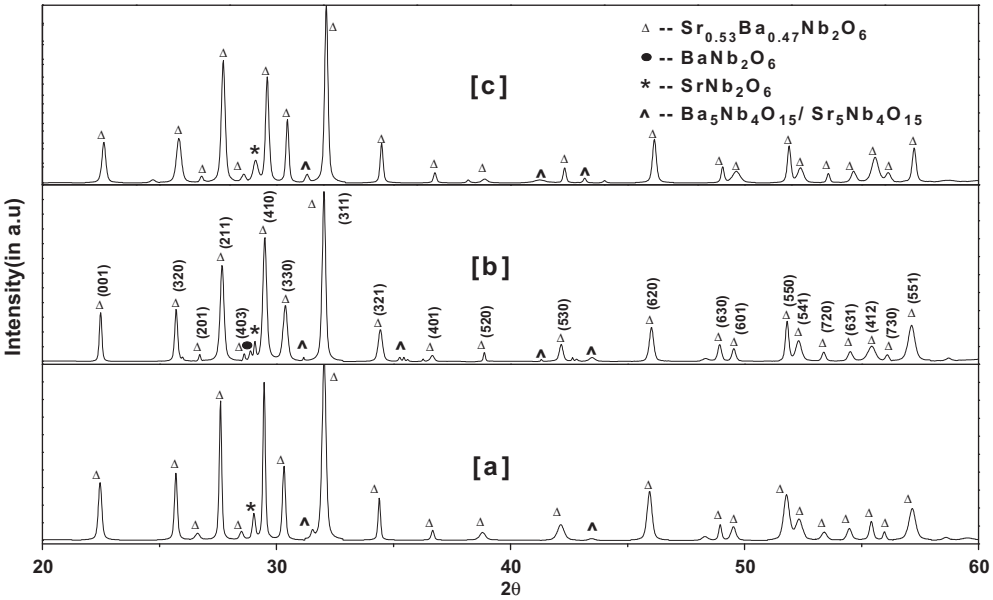

Fig. 2. XRD patterns of SBN53 ceramic powders calcined at 1200 °C for (a) 20 min, (b) 30 min and (c) 45 min.

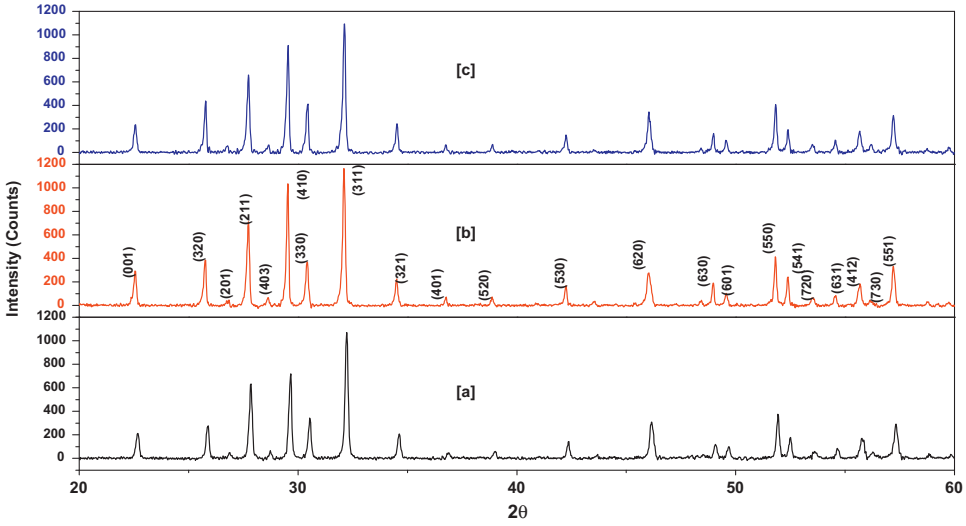

Fig. 3. XRD patterns of SBN53 ceramics sintered at 1300 °C. (a) SBN-30–20, (b) SBN-30–30 and (c) SBN-30–40.

3. Results and discussion

3.1. Crystal structural properties

Fig. 2 shows the XRD patterns of SBN53 ceramic powders calcined at 1200 °C for 20, 30 and 45 min in microwave. The peaks marked ^ correspond to $Ba_5Nb_4O_{15}$ (B_5N_4)/$Sr_5Nb_4O_{15}$ (S_5N_4) and peaks marked * and ● correspond to $SrNb_2O_6$ (SN) and $BaNb_2O_6$ (BN) phases, respectively [23]. SN and BN phases are identified with single prominent XRD peaks. The peaks of BN, SN and SBN phases overlap (since SBN is a solid solution of SN + BN) and not many prominent peaks corresponding to BN and SN phases can be identified in the XRD pattern. Fang et al. [23] have also identified BN and SN phases with the corresponding single prominent XRD peaks. XRD patterns of all the samples show peaks corresponding to SN, B_5N_4/S_5N_4 and SBN53 phases. Whereas, XRD pattern of the powder annealed for 30 min shows the additional peaks corresponding to BN phase. The relative intensity of the peak corresponding to SN phase is found to be ~13.73,9.78 and 11.8% in the powders annealed for 20, 30 and 45 min, respectively. The relative intensity of the peak corresponding to BN phase is found to be ~5.19% in the powder annealed for 30 min. The formation of SBN with tetragonal TTB phase is reported to occur as a reaction process involving following steps [23]:

$$5BaCO_3 + 2Nb_2O_5 \overset{600-900\,^\circ C}{\longrightarrow} Ba_5Nb_4O_{15} + 5CO_2 \quad (1)$$

$$5SrCO_3 + 2Nb_2O_5 \overset{600-900\,^\circ C}{\longrightarrow} Sr_5Nb_4O_{15} + 5CO_2 \quad (2)$$

$$Ba_5Nb_4O_{15} + 3Nb_2O_5 \overset{800-1100\,^\circ C}{\longrightarrow} 5BaNb_2O_6 \quad (3)$$

$$Sr_5Nb_4O_{15} + 3Nb_2O_5 \overset{800-1100\,^\circ C}{\longrightarrow} 5SrNb_2O_6 \quad (4)$$

$$BaNb_2O_6 + SrNb_2O_6 \overset{1000-1150\,^\circ C}{\longrightarrow} 2(Sr_{0.5}Ba_{0.5})Nb_2O_6 \quad (5)$$

The presence of peaks corresponding to intermediate phases indicates the incomplete formation of SBN53 phase which is essential for reactive sintering to occur [19].

Fig. 3 shows the XRD patterns of SBN53 ceramics calcined at 1200 °C for 30 min and sintered at 1300 °C for different durations. Sharp and distinct peaks corresponding to single SBN (TTB) phase are observed in all the samples (i.e. sintered at 1300 °C for 20 min, 30 min and 40 min). Whereas, TTB phase is observed in SBN53 ceramics synthesized by reactive sintering in a conventional heating furnace when sintered at 1250 °C for 5 h [16]. From XRD data, the intensity (in counts)

Table 1
Structural, density and dielectric parameters of SBN53 ceramics synthesized under different microwave processing conditions.

Sample	Lattice parameters		Bulk density (g/cm^3)	Relative density (%)	T_c (°C)	ε_r at 10 kHz	tan δ at 10 kHz
	a (Å)	c (Å)					
SBN-20–20	12.4385	3.9198	4.93	91.65	113	2212	0.008
SBN-20–30	12.4819	3.9424	4.98	93.87	121	1879	0.038
SBN-20–40	12.4371	3.9436	5.10	95.44	125	1944	0.012
SBN-30–20	12.4483	3.9334	5.08	94.97	115	2498	0.010
SBN-30–30	12.4657	3.9354	5.19	97.25	121	2427	0.009
SBN-30–40	12.4856	3.9426	5.22	98.32	134	2286	0.016
SBN-45–20	12.4880	3.9545	4.59	86.75	123	1359	0.005
SBN-45–30	12.4467	3.9401	4.92	92.06	123	1837	0.008
SBN-45–40	12.4867	3.9410	5.07	95.58	125	2350	0.016

of the highest intensity peak (3 1 1) is found to be 1070, 1164 and 1094 for SBN-30–20, SBN-30–30 and SBN-30–40 samples, respectively. This observed decrease in the intensity when the sintering time is increased to 40 min, suggests that the further increase in sintering time would decrease the degree of grain orientation in the ceramics [24]. The driving force for orientation of grains (planes) comes from the size difference between the templates and the equiaxed grains [25]. In the initial stage of sintering, the large driving force results in rapid grain growth and coarsening of equiaxed grains. This decrease in size difference between the grains and the equiaxed grains results in the decrease of degree of grain orientation at longer sintering times [25]. Lattice parameters of all the sintered SBN ceramics were calculated using EXPO2009 [26] and all the specimens were found to be in tetragonal phase belonging to p4bm space group. Table 1 lists the lattice parameters of the SBN53 ceramics synthesized under different conditions.

3.2. Density and surface morphology properties

The effect of sintering time on variation of bulk density is shown in Fig. 4. It is clear that the SBN ceramics which are prepared from powders calcined at 1200 °C for 30 min are denser compared to ceramics calcined at 1200 °C for 20 or 45 min irrespective of the sintering time. The high density observed in case of samples prepared from powders calcined for 30 min can be explained considering the presence of two low temperature melting phases SN and BN and the

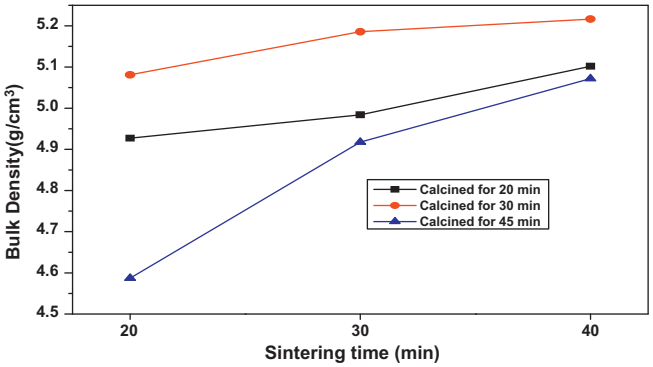

Fig. 4. Density variation of SBN53 ceramics sintered at 1300 °C as a function of sintering time.

intermediate phases B_5N_4 and S_5N_4. The microwave power absorbed per unit volume (P_a) is expressed by

$$P_a = \omega\varepsilon_0\varepsilon'' E^2 + \omega\mu_0\mu'' H^2 \quad (\mathrm{W/m^3}) \tag{6}$$

where E and H are electric and magnetic fields, ω is angular frequency, ε_0 and μ_0 are permittivity and permeability of free space, and ε'' and μ'' are dielectric and magnetic loss factors respectively [27]. Hence, in a microwave furnace, energy is distributed equally over the space of the specimen which enables uniform and rapid heating. Transient liquid phase sintering depends on heating rate [28]. The slower heating rate gives more time for solid-state diffusion prior to liquid phase

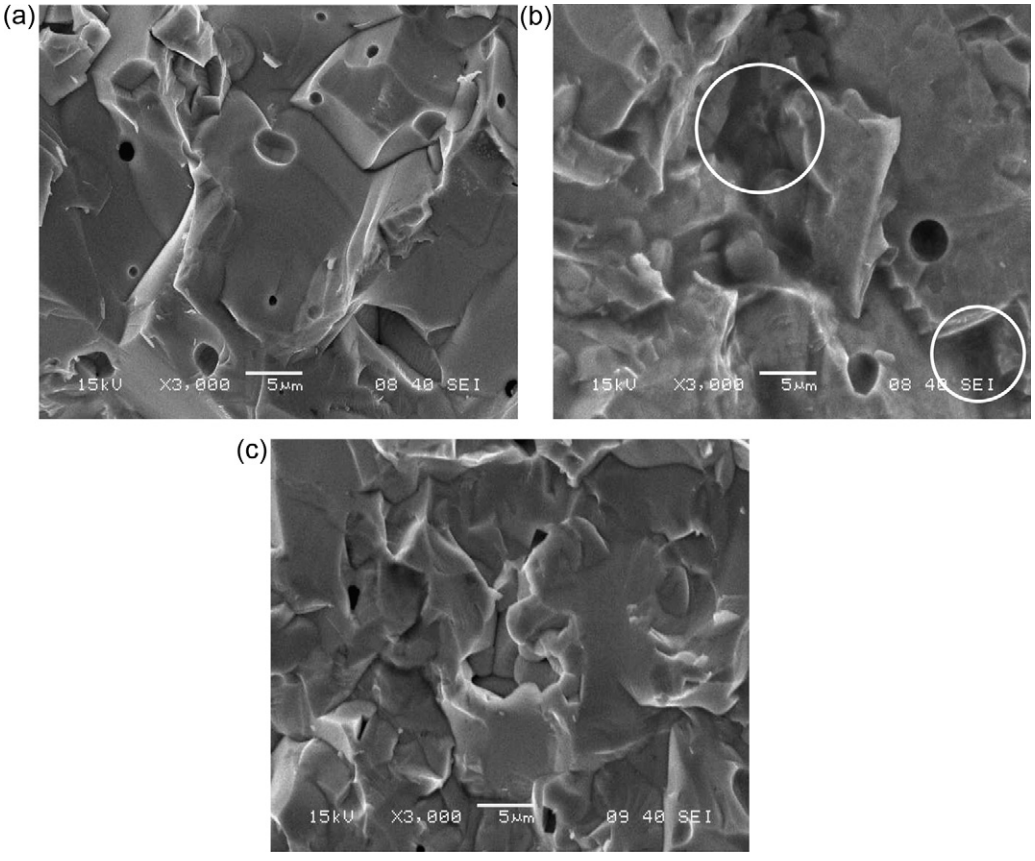

Fig. 5. SEM images of fractured surface of sintered SBN53 ceramics. (a) SBN-20–30, (b) SBN-30–30 and (c) SBN-45–30.

formation and therefore slow heating rate inhibits the liquid phase sintering. Therefore, higher heating rates are beneficial when sintering involves a transient liquid phase. It is a well-established fact that better densification takes place during liquid phase sintering. This acceleration of densification during liquid phase sintering occurs due to a ''wetting'' action of the powder particles by this liquid phase. Creating curved iquid-meniscus surfaces on the particles, capillary forces act and hence draw the particles together. Simultaneously, the wetting agent acts as a lubricant to allow reorientation of the particles into a more compact, dense structure. In addition to heating, the electric field and magnetic field present in microwaves enhance diffusion of atoms/ions [29] and hence better densification. Whereas in conventional heating the heat transfer is from surface to centre of the sample, hence longer durations are required. And there is no electric/magnetic field to supplement the driving force for the diffusion of atoms. It can be concluded that microwave assisted heating simultaneously supplies heat required for reaction and additional driving force required for densification. Table 1 lists the bulk density and relative density of SBN ceramics synthesized under different reactive sintering processing conditions. The relative density of SBN-30–40 is found to be 98.32% (of theoretical density). Whereas, the highest relative density obtained in conventionally processed SBN (with $x = 0.5$) ceramics is 93.6% (of theoretical density) [12]. This indicates that microwave reactive sintering is very effective in obtaining dense ceramics in less processing time.

Fig. 5 shows the SEM morphology of fractured surfaces of SBN53 ceramics calcined for different times and sintered at 1300 °C for 30 min in a microwave furnace. Grain boundary is visible in ceramic samples prepared from the powders calcined at 1200 °C for 20 min and 45 min, whereas in case of ceramic samples prepared from the powders calcined at 1200 °C for 30 min melt phase (circled in Fig. 5b) is observed. From Table 1, it is clear that the porosity is least in case of ceramic samples prepared from the powder calcined at 1200 °C for 30 min. This

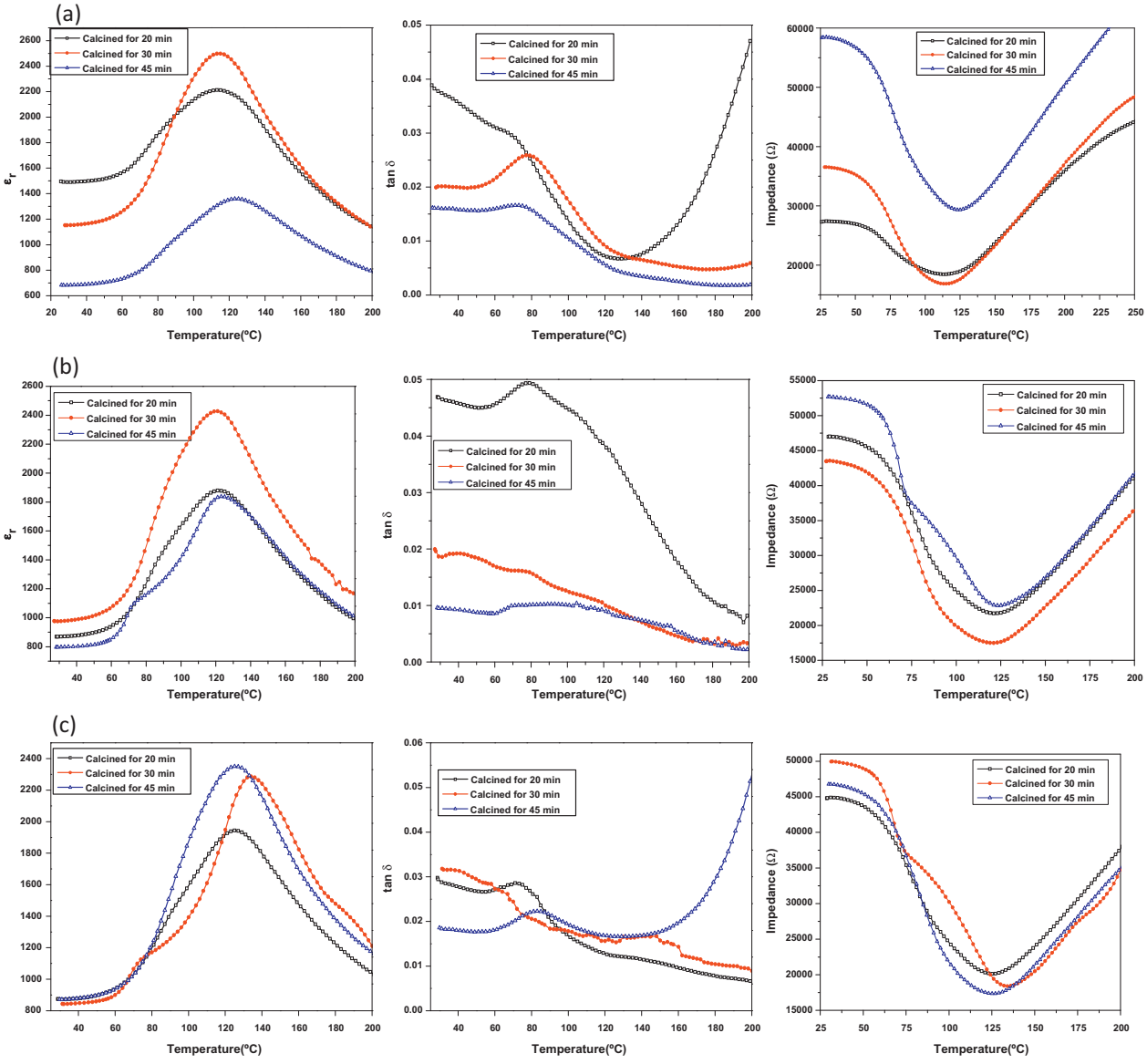

Fig. 6. Variation of ε_r, tan δ and impedance parameters with temperature of SBN53 ceramic samples sintered at 1300 °C for (a) 20 min (b) 30 min and (c) 40 min.

phenomenon observed can be accounted considering the amounts of low temperature melting phases SN and BN in the powders calcined for different durations. The powder calcined for 30 min has two low temperature melting SN and BN phases whereas powders calcined for 20 and 45 min have only one low temperature melting phase. The higher amount of low temperature melting phases in the material calcined at 1200 °C for 30 min enhances liquid phase sintering and helps in better densification. This is also supported by the density measurements of SBN53 ceramic samples.

3.3. Dielectric and ferroelectric properties

Fig. 6 shows the variation of ε_r, tan δ and impedance (Z) parameters with temperature at an applied frequency of 10 kHz of SBN53 ceramic samples sintered at 1300 °C for different durations. The plot of ε_r vs. temperature is a typical behavior of a ferroelectric system, which undergoes phase transition at a temperature called as Curie temperature (T_c). Values of T_c, ε_r and tan δ (at T_c) of SBN53 ceramics are given in Table 1. As can be seen from Fig. 6, T_c increases with the increase in sintering time. The increase in T_c with sintering time can be related to the porosity of ceramics. T_c is proportional to internal stress in the system [30]. The pores help in relieving the internal stress. Therefore, here with the increase in sintering time, the porosity is decreasing and hence increase in internal stress, which gives rise to increase in T_c [30]. From Fig. 6, the value of tan δ is found to decrease with temperature in ceramic samples sintered for 30 min. The samples sintered for 20 and 40 min show a tan δ peak before dielectric T_c, which is generally observed in ferroelectrics [31,32]. From Fig. 6, the value of Z is observed to decrease with temperature up to T_c and increase above T_c in each of the sample. It is known that the dielectric loss is a sum of the relaxation loss of the dipoles and the resistive loss [33].

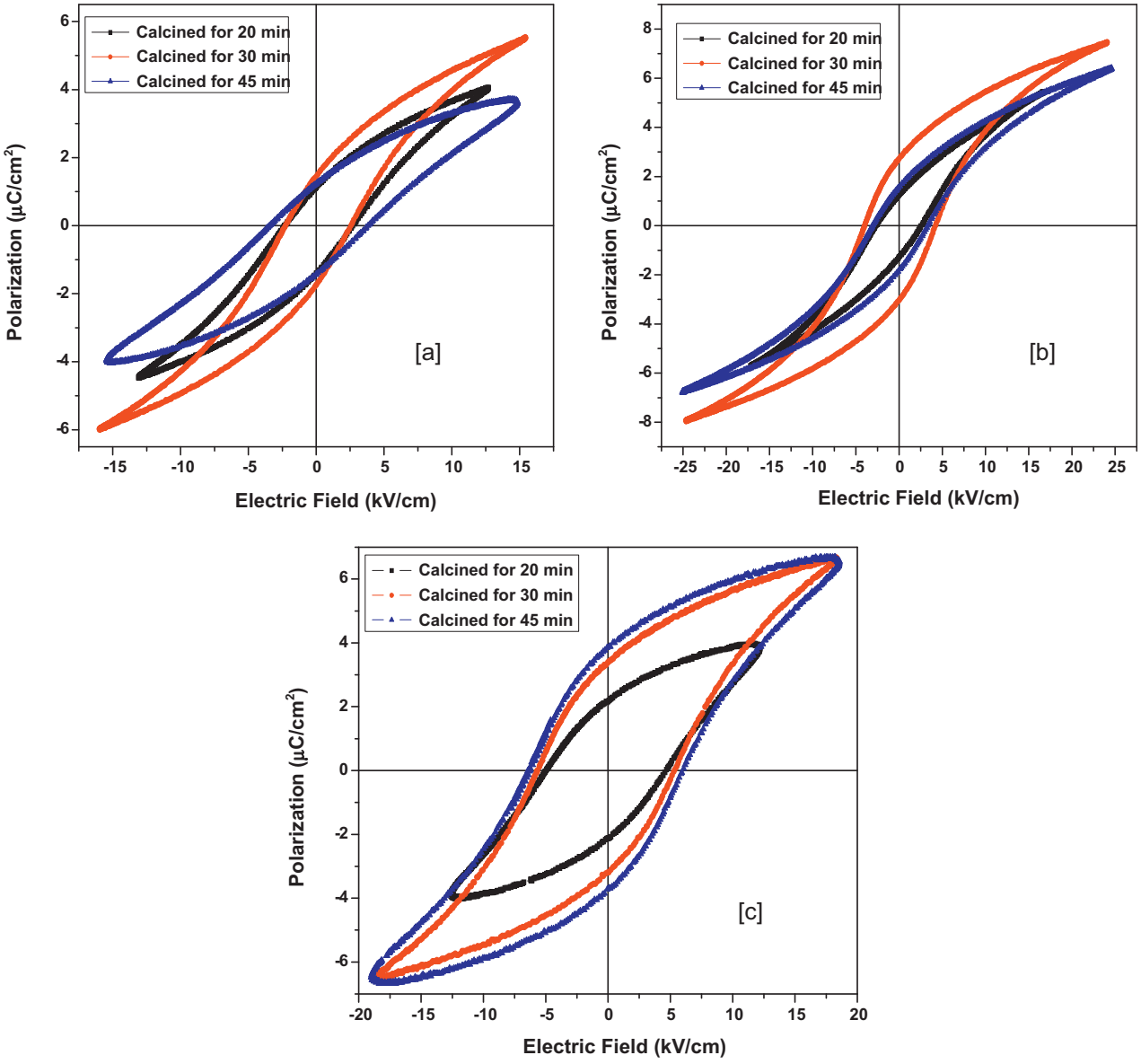

Fig. 7. P–E hysteresis loops of SBN53 samples sintered for (a) 20 min (b) 30 min and (c) 40 min.

The relaxation loss comes from relaxation of the dipoles which expend energy and the resistive loss comes from energy consumed by free carriers generated by oxygen vacancies [34]. The decrease in the value of tan δ with increase in temperature can be a consequence of decrease in relaxation time with temperature [34]. This decrease in relaxation time allows dipoles to be in phase with the applied electric field hence low tan δ. Increase of Z in all samples along with increase in the value of tan δ above 120 °C in the SBN-20–20 and SBN-45–40 samples can be explained considering the following mathematical relations among tan δ, Z, resistance (R) and reactance (X):

$$Mod(Z) = (R^2 + X^2)^{1/2} \quad (7)$$

and

$$\tan\delta = \frac{R}{X} \quad (8)$$

Therefore, the observed increase of Z in all samples hints that either R or X or both are increasing with the increase of temperature above 120 °C. Whereas, observed increase of tan δ in case of SBN-20–20 and SBN-45–40 samples can be due to increase in the value of R due to increased motion of free charge carriers above ~120 °C [35,36].

Fig. 7 shows the P–E hysteresis loops of SBN ceramic samples sintered for different times by microwave process. The development of P–E hysteresis loops confirms the ferroelectric nature of SBN53 ceramic samples synthesized by microwave reactive sintering process. The observed values of P_{sat} ~4.35 μC/cm^2 and P_r ~2.78 μC/cm^2 for SBN-30–30 ceramic sample are higher when compared to the values of P_{sat} ~3.3 μC/cm^2 and P_r ~1.6 μC/cm^2 observed in SBN53 ceramics fabricated by reactive sintering in conventional furnace [16]. It can be observed from Fig. 7 that the tips of the P–E hysteresis loops of SBN-30–20, SBN-30–30 and SBN-30–40 are sharper compared to other calcined times. These sharp tips of P–E hysteresis loops indicate high electrical resistivity [37]. This can be attributed to the high density of SBN53 ceramics prepared from powders which have both SN and BN phases. This is again supported by the higher density of SBN53 ceramic calcined for 30 min. High electrical resistivity in these samples suggests higher electrical breakdown strength.

4. Conclusions

Microwave processing is successfully used for reactive sintering of the SBN53 ceramic samples. The presence of SN and BN phases in green compacts was found to enhance the sintering process. SBN53 ceramics with as low as ~1.7% porosity were obtained when powders calcined at 1200 °C for 30 min and the green pellets were sintered at 1300 °C for 40 min. Dense ceramics were obtained in relatively less processing time and hence less energy consumption compared to conventional methods.

References

[1] K. Uchino, Ferroelectric Devices, Marcel Dekker, New York, 2000.

[2] C. David, T. Granzow, A. Tunyagi, M. Wö hlecke, T. Woike, K. Betzler, M. Ulex, M. Imlau, R. Pankrath, Composition dependence of the phase transition temperature in $Sr_xBa_{1-x}Nb_2O_6$, Phys. Status Solidi A: Appl. Res. 201 (2004) R49–R52.

[3] A.M. Glass, Investigation of electrical properties of $Sr_{1-x}Ba_xNb_2O_6$ with special reference to pyroelectric detection, J. Appl. Phys. 40 (1969) 4699–4713.

[4] M.C. Gupta, The Handbook of Photonics, CRC Press, Boca Raton, 1997.

[5] J.B. Thaxter, Electrical control of holographic storage in strontium-barium niobate, Appl. Phys. Lett. 15 (1969) 210–212.

[6] R.R. Neurgaonkar, W.K. Cory, Progress in photorefractive tungsten bronze crystals, J. Opt. Soc. Am. B: Opt. Phys. 3 (2) (1986) 274–282.

[7] S.T. Liu, R.B. Maciolek, J.D. Zook, B. Rajagopalan, Electro-optic and ferroelectric effect in lanthanum-doped strontium barium niobate single crystals, Ferroelectrics 87 (1988) 265–269.

[8] Y. Xu, H.C. Chen, S.T. Liu, Optical properties and linear electrooptic effect in ferroelectric single crystal KNSBN, Jpn. J. Appl. Phys. 24 (1985) 278–280.

[9] N.S. VanDamme, A.E. Sutherland, L. Jones, K. Bridger, S.R. Winzer, Fabrication of optically transparent and electro-optic strontium barium niobate ceramics, J. Am. Ceram. Soc. 74 (1991) 1785–1792.

[10] E. Rossi, Low level environmental lead exposure – a continuing challenge, Clin. Biochem Rev. 29 (2008) 63–70.

[11] R.R. Neurgaonkar, J.R. Oliver, L.E. Cross, Ferroelectric properties of tetragonal tungsten bronze single crystals, Ferroelectrics 56 (1984) 1035–1040.

[12] P.K. Patro, A.R. Kulkarni, C.S. Harendranath, Dielectric and ferroelectric behavior of SBN50 synthesized by solid-state route using different precursors, Ceram. Int. 30 (2004) 1405–1409.

[13] M. Venet, I.A. Santos, J.A. Eiras, D. Garcia, Potentiality of SBN textured ceramics for pyroelectric applications, Solid State Ionics 177 (2006) 589–593.

[14] N.S. VanDamme, A.E. Sutherland, L. Jones, K. Bridger, S.R. Winzer, Fabrication of optically transparent and electrooptic strontium barium niobate ceramics, J. Am. Ceram. Soc. 74 (1991) 1785–1792.

[15] Q.W. Huang, L.H. Zhu, J. Xu, P.L. Wang, H. Gu, Y.B. Cheng, Effect of V_2O_5 on sintering behaviour, microstructure and dielectric properties of textured $Sr_{0.4}Ba_{0.6}Nb_2O_6$ ceramics, J. Eur. Ceram. Soc. 25 (2005) 957–962.

[16] C. Duran, S.T. McKinstry, G.L. Messing, Fabrication and electrical properties of textured $Sr_{0.53}Ba_{0.47}Nb_2O_6$ ceramics by templated grain growth, J. Am. Ceram. Soc. 83 (2000) 2203–2213.

[17] W.J. Lee, T.T. Fang, Densification and microstructural development of the reaction sintering of strontium barium niobate, J. Am. Ceram. Soc. 81 (1998) 1019–1024.

[18] P.K. Patro, A.R. Kulkarni, S.M. Gupta, C.S. Harendranath, Improved microstructure, dielectric and ferroelectric properties of microwave-sintered $Sr_{0.5}Ba_{0.5}Nb_2O_6$, Physica B 400 (2007) 237–242.

[19] W.S. Hong, L.C. Dejonghe, X. Yang, M.N. Rahaman, Reaction sintering of ZnO–Al_2O_3, J. Am. Ceram. Soc. 78 (1995) 3217–3224.

[20] M.N. Rahaman, H.E. L.C. Dejonghe, Reaction sintering of zinc ferrite during constant rates of heating, J. Am. Ceram. Soc. 76 (1993) 1739–1744.

[21] N.S. Stoloff, D.E. Alman, Powder processing of intermetallic alloys and intermetallic matrix composites, Mater. Sci. Eng. A 144 (1991) 51–62.

[22] D.K. Agarwal, Microwave processing of ceramics, Curr. Opin. Solid State Mater. Sci. 3 (1998) 480–485.

[23] T.T. Fang, N.T. Wu, FUH-SHAN SHIAU Formation mechanism of strontium barium niobate ceramic powders, J. Mater. Sci. Lett. 13 (1994) 1746–1748.

[24] B.D. Cullity, Elements of X-ray Diffraction, Addison-Wesley, Reading, MA, 1979.

[25] H. Yilmaz, G.L. Messing, S. Trolier-Mchinstry, (Reactive) Templated grain growth of textured sodium bismuth titanate ($Na_{1/2}Bi_{1/2}TiO_3$–$BaTiO_3$) ceramics-I. Processing, J. Electroceram. 11 (2003) 207–215.

[26] A. Altomare, M. Camalli, C. Cuocci, C. Giacovazzo, A. Moliterni, R. Rizzi, EXPO2009: structure solution by powder data in direct and reciprocal space, J. Appl. Cryst. 42 (2009) 1197–1202.

[27] D. Agrawal, Microwave Sintering of ceramics, composites and metal powders, in: Z.Z. Fang (Ed.), Sintering of Advanced Materials, Woodhead Publishing, UK, 2010, pp. 222–248.
[28] D.M. Sims, A. Bose, R.M. German, Reactive sintering of nickel aluminide, Prog. Powder Metall. 43 (1987) 575–596.
[29] Y.V. Bykov, S.V. Egorov, A.G. Eremeev, K.I. Rybakov, V.E. Semenov, A.A. Sorokin, S.A. Gusev, Evidence for microwave enhanced mass transport in the annealing of nanoporous alumina membranes, J. Mater. Sci. 26 (2001) 131–137.
[30] P. Kumar, C. Prakash, T.C. Goel, Dielectric and electrostrictive properties of PMNT near MPB, Sci. Technol. Adv. Mater. 8 (2007) 463–468.
[31] Y.N. Wang, Y.N. Huang, Mechanical and dielectric loss related to ferroelectric and relaxor phase transitions and domain walls, J. Alloys Compd. 211–212 (1994) 356–360.
[32] L.N. Kamysheva, S.N. Rozhdin, The peculiarities of the electrophysical properties of the potassium dihydrogen phosphate (KDP) group crystals connected with the domain structure dynamics, Ferroelectrics 71 (1987) 281–296.
[33] P. Li, J.F. McDonald, T.M. Lu, Densification induced dielectric properties change in amorphous barium titanate thin films, J. Appl. Phys. 71 (1992) 5596–5600.
[34] K. Kumar, B.K. Singh, M.K. Gupta, N. Sinha, B. Kumar, Enhancement in dielectric and ferroelectric properties of lead free $Bi_{0.5}(Na_{0.5}K_{0.5})_{0.5}TiO_3$ ceramics by Sb-doping, Ceram. Int. 37 (2011) 2997–3004.
[35] C. Indrani, A.K. Jha, S.K. Agarwal, Structural, dielectric and electrical studies in tungsten doped $SrBi_2Ta_2O_9$ ferroelectric ceramics, Ceram. Int. 33 (2007) 41–47.
[36] D.K. Pradhan, R.N.P. Chaudhary, B.K.Y. Samantara, Studies of dielectric relaxation and AC conductivity behavior of plasticized polymer nanocomposite electrolytes, Int. J. Electrochem. Sci. 3 (2008) 597–608.
[37] G.H. Heartling, Ferroelectric ceramics: history and technology, J. Am. Ceram. Soc. 82 (1999) 797–818.